Cold Regions Science and Technology, 22 (1993) 47–63
Elsevier Science Publishers B.V., Amsterdam

A constitutive model of saturated soils for frost heave simulations

Radoslaw L. Michalowski
Department of Civil Engineering, The Johns Hopkins University, Baltimore, MD 21218, USA

(Received 11 November 1991; accepted after revision 15 February 1993)

ABSTRACT

It is argued that the volume increase of frost-susceptible soils due to ice growth during freezing can be described by a phenomenological model without resorting to the micromechanical processes causing the ice growth. Judging from solid mechanics' experience, such model may prove to be more accurate in predictions of frost heave than models based on micromechanical processes (single ice lens formation). A particular model based on a porosity rate function is described. This approach, suggested earlier by Blanchard and Frémond (1985), is extended to include more factors affecting ice growth during freezing of frost susceptible soils. Results of simulations of a one-dimensional freezing process are shown to illustrate the main features of the model and its potential applicability. Although a quantitative verification of the model was not possible, as sufficient data from lab tests were not available to calibrate it, the numerical results indicate a very realistic response of samples to simulated freezing processes.

1. Introduction

While the significant findings related to frost heave in soils were published more than half a century ago (Taber, 1929, 1930; Beskow, 1935), intensive efforts to rigorously describe the process of soil freezing and the related frost heave did not start until about three decades later. The capillary theory of frost heaving (e.g., Penner, 1959; Everett, 1961), based on the Laplace surface tension equation, became popular in the 1960's and 1970's. The simplicity of the capillary theory was appealing, but experimental tests did not confirm its validity: heaving pressures during freezing tests were found to be significantly larger than those predicted by the theory. There was also evidence that ice lenses can form within frozen soil at some distance from the freezing front, which could not be explained by the capillary theory. These shortcomings led to the concept of secondary heaving, primary heaving being assigned to the capillary action.

The secondary heaving mechanism was proposed by Miller (1978). The secondary frost heave theory is based on a regelation mechanism, which causes the movement of particles imbedded in ice under a temperature gradient. A key experiment presenting the migration of particles in ice up the temperature gradient was shown by Römkens and Miller (1973). Pore ice and ice lenses are treated as one body in the secondary heave mechanism. Due to kinematical constraints, the mineral (solid) particles do not move up the temperature gradient, and thus it is the ice which moves down the temperature gradient, the relative particle–ice motion being the same. This mechanism gives rise to secondary frost heave, and its mathematical description is often called the *rigid ice model*. Attempts at practical calculations of frost heave using the rigid ice model can be found in papers by O'Neill and Miller (1980, 1985), Holden (1983), Holden et al. (1985), and Black and Miller (1985).

Perhaps the *rigid ice model* received the most at-

0165-232X/93/$06.00

tention in the literature, though other useful models can be found (e.g., Konrad and Morgenstern, 1980; Guymon et al., 1984; Shen and Ladanyi, 1987). The model of Konrad and Morgenstern (1980), though not as widely accepted by the scientific community as the rigid ice model, has proven to be a more useful tool for engineering purposes (see e.g., Konrad and Morgenstern, 1984; Nixon, 1987). A common characteristic of the aforementioned models is that they all consider the process of freezing at the microscopic level (i.e., they consider micromechanical processes between the components of the mineral–ice–water mixture). The Clausius–Clapeyron equation is then utilized to relate pressure to temperature at the water–ice interface. Little attention has been paid to constitutive modelling of soils, where frost susceptibility is defined as a property of the mineral–ice–water composite. Such "macroscopic" approach to modelling of frost susceptible soils was suggested by Blanchard and Frémond (1985). The same concept is used in this paper, though with a modified function representing the rate of porosity increase during freezing, to obtain a more realistic response of the soil to freezing.

As the "macroscopic" approach to modelling frost heave in soils is not widely accepted, the philosophy behind this approach is presented in the next section. The following two sections present the porosity rate function and the unfrozen water content. Fundamental equations of the model are then presented in section 5. Simulations and sensitivity of the simulated heave processes to the characteristic material parameters are discussed in section 6. Remarks and conclusions are given last.

2. Philosophy of the approach

It is the model of secondary heaving (or rigid ice model) which has received the most attention in the scientific community. However, the current stage of development of this model allows only a one-dimensional freezing simulation. Like the model based on capillary action, the secondary frost heave model is based on considering the micromechanical processes, and the heaving effect is obtained as the integral of the growth of all ice lenses in the frozen column (1-D process). The term "micromechanical" here pertains to processes taking place among the components of the soil skeleton–ice–water mixture. Macromechanical (or global) effects are those seen as the response of the whole mixture (e.g., porosity increase).

Constructing a model for predictions of frost heave based on the summation of the actual micromechanical processes will, certainly, lead to realistic qualitative results. As to the quantitative results, the micromechanical approach may not necessarily be the most reliable one. This has certainly been true in the mechanics of solids, where phenomenological models based on introducing material parameters at the macroscopic level were far more successful than micromechanics-based models in predicting such global quantities as displacements and limit loads. The simplest examples of constitutive (of phenomenological) models are Hook's model of linear elasticity, and the model of perfect plasticity. As opposed to micromechanics-based models, they cannot explain why the deformation is elastic (or plastic), but they can be quite accurate in determining the magnitudes of deformation or the stress state, given material properties defined at the macroscopic level (Young's modulus, Poisson's ratio, or the yield condition and the flow rule). Micromechanical models can explain the nature of the deformation, but the quantitative predictions are usually orders of magnitude apart from the true result.

There is no reason to doubt that a phenomenological model formulated on the macroscopic level can be constructed for frost susceptible soils so the increase of porosity due to ice lens formation can be modelled. While the material functions defined at the macroscopic level do not have to be derived from microscopic processes, their mathematical form must reflect the experimentally observed effect. For frost susceptible soil model this effect is the increase in volume which will be modelled by a *porosity rate function*, $\dot{n}$, as suggested earlier by Blanchard and Frémond (1985). This concept is extended here to include more factors influencing growth of ice during the freezing process of soils. Thus the ice growth will be described as the average increase in porosity (volume) of the soil element, rather than as separate ice lens growth.

The frost heave itself is a process which occurs when the frost susceptible soil is placed under cer-

tain conditions. Thus, frost heave can be calculated as the solution to a boundary value problem in which the soil is subjected to specific initial and boundary conditions. While frost susceptibility (expressed by function $\dot{n}$) is a material property, frost heave is a process related to a soil mass and specific boundary conditions rather than to a soil element. In this sense, frost heave itself is not a property of the material, but frost susceptibility is.

To formulate and solve the problem of frost heave for specific thermal and hydraulic conditions, constitutive functions in addition to $\dot{n}$ need to be adopted: the unfrozen water content in frozen soil, the heat transfer and mass flow laws, and the rule describing deformability (and/or yielding) of the soil skeleton and the frozen composite. These equations, along with the fundamental principles of energy, mass, and momentum conservation, form the set of equations to be solved for given boundary conditions to obtain frost heave.

Related to the approach proposed is the interpretation of the freezing soil as a *heat engine*. Heaving soil performs mechanical work against external loads (gravity and boundary forces), and also performs work which is either dissipated (e.g., during plastic deformation of the skeleton) or stored as elastic energy (in both ice and skeleton). Thus it can be argued that part of the latent heat released when water freezes is transformed into mechanical work by means of a specific heat engine of a very low efficiency. While the temperature gradients at the macroscopic level are considered finite within the freezing soil, the specific conditions for the heat engine must exist at the microscopic level.

As all functions are formulated on the macroscopic level, this approach does not utilize the Clausius–Clapeyron equation which is used in the micromechanics-based approach (analysis of a single ice lens formation). Specific equations are presented in the next three sections.

3. Porosity rate function

According to the approach taken, the formation of a single ice lens is not attempted here; instead, the average volume increase of the soil matrix–water–ice mixture is considered due to the ice growth. This volume increase is modelled with a *porosity rate function*, $\dot{n}$. The porosity rate function must account for characteristic features of the freezing process of frost susceptible soils, as known from laboratory tests. In particular, it must be a function of temperature, temperature gradient, porosity, and the stress state. The following form of the porosity rate function is proposed

$$\dot{n}=\dot{n}_{\mathrm{m}}\frac{T-T_0}{T_{\mathrm{m}}}\exp\left(1-\frac{T-T_0}{T_{\mathrm{m}}}\right)\left(1-\exp\left(\alpha\frac{\partial T}{\partial l}\right)\right)(1-n)^{\beta}\exp\left(-\frac{\overline{\sigma_{kk}}}{n\zeta}\right);\qquad T<T_0,\quad \frac{\partial T}{\partial t}<0 \tag{1}$$

where $\dot{n}$ is the porosity rate ($\partial n/\partial t$), n is the porosity, T is the temperature of the composite (in °C), and $\overline{\sigma_{kk}}$ is the first invariant of the stress tensor in the frozen composite (compression positive). Parameters $\dot{n}_{\mathrm{m}}$ and T_{m} are the maximum porosity rate and the temperature (in °C) at which that maximum occurs, respectively, and T_0 is the freezing temperature; α, β, and ζ are the material parameters. Note that the function in Eq. (1) does not explicitly depend on hydraulic conductivity. This conductivity is implicitly included in other material parameters.

The porosity rate function here is constructed in such a way that its first part, containing $\dot{n}_{\mathrm{m}}$ and T_{m}, describes the porosity rate as a function of temperature (Fig. 1a), while the two expressions in parentheses and the last exponential function are dimensionless factors, all ranging from 0 to 1.0, depending on the temperature gradient, current porosity, and the stress state, respectively. The analytical form of these factors was selected in such a way so that the tendency of frost heave with increase/decrease in $\partial T/\partial l$, n, and $\overline{\sigma_{kk}}$ (as known from the lab tests) is captured, and only one extra material parameter is introduced to describe each effect. The inhibiting effect of the temperature gradient, porosity, and the stress state on the porosity growth is illustrated in Figs. 1b–d.

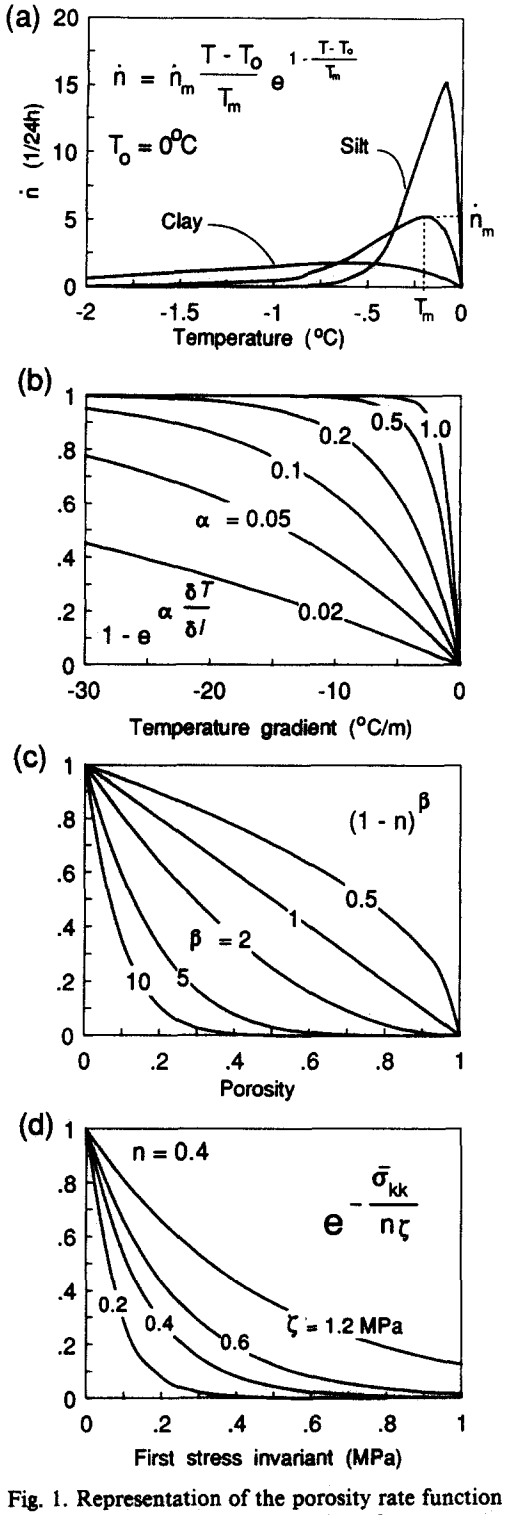

Fig. 1. Representation of the porosity rate function components: (a) porosity rate as a function of temperature; (b) influence of the temperature gradient; (c) influence of porosity; (d) influence of the stress-state.

3.1. *Influence of temperature*

The first part of Eq. (1), containing two material parameters, $\dot{n}_m$ and T_m, is almost identical to that proposed by Frémond (1987), who suggested that the porosity rate function be proportional to a material constant, temperature, and the exponential function with the temperature and another material constant: $\dot{n} = -aTe^{bT}$. This function may be written in terms of $\dot{n}_m$ and T_m (Fig. 1a), and for an arbitrary freezing temperature T_0 as in Eq. (1). The hypothesis of a maximum porosity increase as a material property comes from the fact that hydraulic conductivity decreases drastically with a decrease in temperature while suction increases. It is then likely that the influx of water into a freezing soil element has a maximum at some temperature below freezing temperature T_0. The growth of ice behind the freezing front (related to non-Darcian mass transport) takes place at temperatures further below T_m.

At freezing temperature $T = T_0$ no ice growth takes place ($\dot{n} = 0$); the porosity rate increases rapidly with the decrease in temperature, reaches a maximum, and diminishes to quantities near zero for temperatures well below zero. The rapid increase of porosity at temperatures slightly below T_0 can be interpreted as primary frost heave, while its slow growth at lower temperatures can be interpreted as the secondary frost heave process.

Parameters $\dot{n}_m$ and T_m allow the simulation of cases known from laboratory experiments. For example, silt exhibits a relatively high rate of heave (high porosity rate) at temperatures slightly below zero, but it diminishes quickly when the unfrozen water content drops down and the hydraulic conductivity becomes very small (Fig. 1a); clay, on the other hand, under the same boundary conditions, heaves more slowly, but the rate of heave does not drop as rapidly with a decrease in temperature.

A simulation of a boundary value problem with porosity rate being modelled by only this first part of Eq. (1) was shown by Li et al. (1989).

3.2. *Temperature gradient*

The second component of the porosity rate function, $(1 - e^{\alpha(\partial T/\partial l)})$, involves the temperature gra-

dient along the heat flow lines (maximum magnitude of gradient). Co-ordinate l coincides with the tangent to heat flow lines and is directed toward the cold side of the freezing front, hence $\partial T/\partial l < 0$. For a sufficiently large magnitude of thermal gradient, this function becomes close to unity, Fig. 1b, and it drops to zero when the magnitude of the thermal gradient drops to zero. The value of 1 is the limit for the coefficient representing the inhibiting effect of the temperature gradient, and not the limit for the porosity rate itself. Assuming that cryogenic suction for a given soil is a function of temperature alone, the suction gradient must be zero when $\partial T/\partial l = 0$. According to Darcy's law, no water influx due to cryogenic suction is then possible when $T = \text{const}$. However, water flow is possible through the frozen soil at a constant temperature due to an "externally applied" hydraulic gradient (Burt and Williams, 1976); this flow is neglected here as small relative to that caused by the cryogenic suction gradient.

Dependence of frost heave on the temperature gradient is also an essential part of the segregation potential model, where the water influx into the freezing zone is made proportional to $\partial T/\partial l$ and segregation potential SP.

3.3. *Influence of porosity*

The term $(1-n)^\beta$ in Eq. (1) makes the porosity rate a function of the current value of porosity. Without getting into the details of a single ice lens growth, the process can take place only if both water and a solid soil skeleton are present. An increase in porosity at a given temperature below freezing causes an increase in the relative ice content, $\theta^{(i)}$, while the relative unfrozen water content, $\theta^{(w)}$, and the solid content, $\theta^{(s)}$, drop (quantities θ are defined in Eq. 3). This leads to a decrease in the hydraulic conductivity, and, consequently, to a drop in the water supply. When porosity becomes close to unity, the soil skeleton may be considered as particles embedded in ice, and the increase of the ice volume due to the Darcian influx of water is stopped, since the hydraulic flow paths in the soil–skeleton–ice mixture are discontinuous. At the limit, $n = 1$, the ice fills the whole volume and no further increase is possible. Note that the non-Darcian water and ice transport due to the regelation phenomenon (secondary frost heaving) also requires that the porosity be less than 1. The process cannot take place in the absence of a skeleton and unfrozen water.

3.4. *Influence of the stress state*

The influence of the stress state in soil on ice lens formation, simulated here as an increase in porosity, is perhaps one of the more crucial elements in phenomenological modelling of frost heave. Considering the stress state on the microscopic level, it is the stress in ice which is likely to be the governing parameter (Williams and Wood, 1985).

There has been very little concern, so far, regarding the stress state in freezing soil and its role in modelling frost susceptible soils. If considered at all, it is usually included as "the influence of the overburden pressure", which, from the standpoint of constitutive modelling, is not acceptable. The "overburden pressure" is a boundary condition (part of the boundary value problem) and cannot influence the constitutive model of the material itself; it is the stress state at the point of consideration which influences the behavior of the material at that point. In general, there is an infinite number of stress boundary conditions causing the same stress state at a given point. Successful use of the "overburden pressure" as a parameter in some models comes from the fact that these models are restricted to one-dimensional deformation processes, where the normal stress component in the direction of the overburden pressure throughout the soil is statically determinate and equal to the overburden pressure plus the weight of the material above the point of consideration.

Following the mixtures theory, the total stress in the mineral–ice–water mixture $\overline{\sigma_{ij}}$ is

$$\overline{\sigma_{kl}} = \theta^{(s)}\sigma_{kl}^{(s)} + \theta^{(i)}\sigma_{kl}^{(i)} + \theta^{(w)}u\delta_{kl} \tag{2}$$

where θ and σ_{kl} are the volumetric fractions and microstresses in the respective constituents, u is the pressure in the water, and δ_{kl} is Kronecker's symbol. Quantities $\theta^{(s)}$, $\theta^{(w)}$, and $\theta^{(i)}$ are defined as

$$\theta^{(s)} = \frac{V^{(s)}}{V} = 1-n, \quad \theta^{(w)} = \frac{V^{(w)}}{V} = \nu n, \quad \theta^{(i)} = \frac{V^{(i)}}{V} = n(1-\nu) \tag{3a}$$

where $V^{(s)}$, $V^{(w)}$, and $V^{(i)}$ are the volumes of the soil skeleton, unfrozen water, and ice, respectively, and $V=V^{(s)}+V^{(w)}+V^{(i)}$, and ν is the unfrozen water concentration in frozen soil

$$\nu=\frac{V^{(w)}}{V^{(i)}+V^{(w)}} \tag{3b}$$

Introducing macrostresses related to the cross-section of the entire composite (symbols with bars), Eq. (2) can be rewritten as

$$\overline{\sigma_{kl}}=\overline{\sigma_{kl}^{(s)}}+\overline{\sigma_{kl}^{(i)}}+\bar{u}\delta_{kl} \tag{4}$$

It follows then, that under a zero external load $\overline{\sigma_{kl}}$, the buildup of stress in ice, $\overline{\sigma_{kl}^{(i)}}$, must be compensated for by the stress in the skeleton, $\overline{\sigma_{kl}^{(s)}}$ (assuming $\bar{u}$ unchanged). Thus the buildup of the compressive stress increment in ice causes a tension increment in the skeleton. Williams and Wood (1985) also gave a similar interpretation of the "heave pressure" transfer. This is possible if the soil skeleton forms a continuous matrix, and the matrix has enough strength to withstand the tensile stresses. Ice inclusions, however, reduce the ability of the skeleton to resist tension, and local slip between mineral particles (plastic flow) can be expected when the ice pockets (lenses) increase their volume. The stress state in the clusters of the soil skeleton is expected to be non-homogeneous and dependent on the geometrical configuration of these clusters with respect to growing ice. The strength of the frozen silt or clay is, of course, much higher than that of the unfrozen soil. However, this is the strength of the mineral–water–ice composite. The strength of the skeleton matrix alone against expansion caused by the growing ice probably changes little with freezing. The average stress state in the skeleton, $\overline{\sigma_{kl}^{(s)}}$, over a representative frozen soil element can presumably be described by a function similar to the yield functions of plastic materials, and the level of tensile strength is probably quite low (comparable to that following from the Mohr–Coulomb yield condition in a tensile regime, for unfrozen silt and clay of comparable liquid moisture content).

Knowing the constitutive relations for the total composite and the soil skeleton, $\overline{\sigma_{kl}}$ and $\overline{\sigma_{kl}^{(s)}}$ can be calculated under a given porosity increase, and u can be back-calculated from Darcy's law. Thus, theoretically, $\overline{\sigma_{kl}^{(i)}}$ can be obtained from Eq. (4). Such estimate of the stress in ice, though theoretically consistent with the model, may be inaccurate, since u is very sensitive to hydraulic conductivity, which changes with temperature. Therefore, the fourth factor in the porosity rate function postulated here reflects the influence of the total stress state in the frozen soil: $\exp(-\overline{\sigma_{kk}}/n\zeta)$, where $\overline{\sigma_{kk}}$ is the first invariant of the stress state in the composite ($\overline{\sigma_{kk}}=\overline{\sigma_{11}}+\overline{\sigma_{22}}+\overline{\sigma_{33}}$), n is the porosity, and ζ is a material parameter. Note that the influence of the stress state is considered without introducing the notion of a frost heave shut-off pressure.

Although the influence of the stress state in ice alone would be physically more justifiable, the inaccuracies in determining $\overline{\sigma_{kl}^{(i)}}$ would make the calculations less reliable. Note that all available attempts at including the influence of the stress state are in terms of the overburden pressure, and thus the total stress.

The decrease in porosity rate $\dot{n}$ with increasing stress is introduced here on the basis of a purely theoretical argument. In order for the material to increase its porosity and cause frost heave, mechanical work has to be done against the external forces (gravity and boundary forces). The dissipation of mechanical energy will also occur during irreversible deformation of some mixture components, and energy will be stored during reversible deformation. This requires that part of the latent heat released when water freezes is changed into mechanical work. Frost heave can then be interpreted as a result of the action of a particular *heat engine*. Macroscopically, the temperature gradients are considered finite, but, for the heat engine to have efficiency larger than 0, a temperature discontinuity must occur at the microscopic level *, otherwise all heat will be diffused. As long as the conditions for the heat engine exist at the microscopic level, part of the latent heat (small, however, due to very low efficiency) will be used to perform the mechanical work. The power made available by the heat engine must then lead to heave

*For example, efficiency of the Carnot heat engine for an ideal gas is: $\mu=1-T_1/T_2$, where T_1 and T_2 are temperatures (in K) of the two heat reservoirs, with T_2-T_1 being the temperature discontinuity.

rates where the higher the confining pressure, the lower the heave rate. This relation is not linear due to dissipation and energy storage terms in the energy balance, and also due to possible structural changes at the microscopic level leading to changes in heat engine efficiency.

3.5. Porosity growth tensor

Porosity changes are described here as scalar $\dot{n}$ (Eq. 1). To capture the anisotropic character of the void growth (due to ice lens formation), the *porosity growth tensor* is introduced

$$\dot{n}_{kl}=\dot{n}\begin{vmatrix}\xi & 0 & 0\\ 0 & \frac{1}{2}(1-\xi) & 0\\ 0 & 0 & \frac{1}{2}(1-\xi)\end{vmatrix} \qquad k,l=1,2,3 \qquad (5)$$

where x_1 coincides with the heat flow lines across the freezing soil element under consideration, and $0.33\leqslant\xi\leqslant 1.0$. The two limit values of ξ (0.33 and 1.0) describe the isotropic growth and unidirectional growth of ice lenses (in the direction of heat flow lines), respectively. Note that $\dot{n}_{kl}$ is identical to the strain rate tensor for the entire frozen composite due to ice growth.

4. Unfrozen water content

In addition to the porosity rate function, $\dot{n}$, the relation representing the unfrozen water content in the frozen soil, w, is important in the model presented. Based on experimental tests (e.g., Anderson and Tice, 1973) the form of this function is assumed as

$$w=w^*+(\bar{w}-w^*)e^{a(T-T_0)} \quad T<T_0,\ \frac{\partial T}{\partial t}<0 \qquad (6)$$

where w is the unfrozen water content as a fraction of the dry weight, w^* is the residual unfrozen water content at some very low reference temperature, $\bar{w}$ is the minimum unfrozen water content at freezing temperature T_0, and a is the third material parameter. Note that this function is different from that proposed by Anderson and Tice (1973) which tends to infinity at freezing temperatures, and thus is unacceptable in numerical calculations. This paper considers only the freezing process; during a thawing process the unfrozen water content can also be expressed by Eq. (6), but parameters $\bar{w}$ and a are likely to be different for both processes.

5. Fundamental equations

The proposed model considers soil a porous medium, with pores filled with water, or water and ice. Volumetric changes occur due to porosity increase, which is caused by the inflowing and freezing water driven by cryogenic suction gradient. The process of the formation of discrete ice lenses is "smeared" over a representative volume, and simulated by the porosity increase of the mixture. The porosity increase is governed by Eq. (1). This function describes the effect on the macroscopic level. While such model cannot explain physical phenomena leading to frost heave, it is expected to be a reliable predictor of frost heave, provided the material parameters are derived from reliable experimental tests.

For unfrozen saturated soil the water content is uniquely determined by porosity

$$w=\frac{\gamma^{(w)}}{\gamma^{(s)}}\frac{n}{1-n} \qquad (7)$$

where $\gamma^{(s)}$ and $\gamma^{(w)}$ are the specific weights of the soil skeleton and water, respectively. Introducing the densities of the three components of the mixture as $\rho^{(s)}$, $\rho^{(w)}$, and $\rho^{(i)}$, respectively, the density of the mixture can be written as

$$\begin{aligned}\bar{\rho}&=\theta^{(s)}\rho^{(s)}+\theta^{(w)}\rho^{(w)}+\theta^{(i)}\rho^{(i)}\\ &=(1-n)\rho^{(s)}+\nu n\rho^{(w)}+n(1-\nu)\rho^{(i)}\end{aligned} \qquad (8)$$

The heat capacity of the mixture per unit volume can be expressed as

$$\begin{aligned}C=(1-n)\rho^{(s)}C^{(s)}&+\nu n\rho^{(w)}C^{(w)}\\ &+n(1-\nu)\rho^{(i)}C^{(i)}\end{aligned} \qquad (9)$$

where $C^{(s)}$, $C^{(w)}$, and $C^{(i)}$ are the mass heat capacities of the soil skeleton, water, and ice, respectively. Due to changing proportions of the components in the freezing soil, the heat capacity will vary.

The Fourier law of heat conduction is adopted

$$Q_i=-\lambda(T)\frac{\partial T}{\partial x_i} \qquad i=1,2,3 \qquad (10)$$

where Q_i is the heat flux vector, T is the temperature, and x_i is the space co-ordinate. Thermal conductivity $\lambda(T)$ is a function of temperature, and it pertains to the conductivity of the soil–water–ice mixture. Water transport is described by Darcy's law

$$q_i = -k(T)\frac{\partial h}{\partial x_i} \qquad i=1,2,3 \tag{11}$$

where q_i is the flow rate vector, h is the hydraulic head, and $k(T)$ is the hydraulic conductivity (function of temperature).

The total stress in the composite, $\overline{\sigma_{kl}}$, is described by Eq. (4). The constitutive relation for the frozen mixture is not specified here in detail. It is only suggested that it may be described with a hypoelastic-type relation

$$\overline{\sigma_{ij}} = B(T)_{ijkl}\overline{\epsilon_{kl}} \qquad i,j,k,l=1,2,3 \tag{12}$$

where $\overline{\epsilon_{kl}}$ is the strain tensor, and $B(T)_{ijkl}$ is the constitutive tensor of the composite. A similar relation describes the deformability of the skeleton itself

$$\overline{\sigma_{ij}^{(s)}} = B(T)_{ijkl}^{(s)}\overline{\epsilon_{kl}^{(s)}} \qquad i,j,k,l=1,2,3 \tag{13}$$

where $\overline{\epsilon_{kl}^{(s)}}$ is the strain tensor and $B(T)_{ijkl}^{(s)}$ is the constitutive tensor of the skeleton. Note that the strain tensor of the composite, $\overline{\epsilon_{kl}}$, is equal to the macrostrain tensor in the skeleton, $\overline{\epsilon_{kl}^{(s)}}$ (compatible deformation). If the deformation process takes place only due to changing porosity, the two strain tensors are equal to the time integral of the porosity growth tensor in Eq. (5).

Equations (1), (5), (6), and (10)–(13) describe the constitutive model of frost susceptible soil. Frost heave, however, is a process dependent on the initial and boundary conditions, and can be described only as a boundary value problem. The solution to the boundary value problem requires that the unknown functions T, h, $\overline{\sigma_{kl}}$, and $\overline{\sigma_{kl}^{(s)}}$ be found such that the fundamental principles of energy, mass, and momentum conservation are satisfied. Using Eq. (10), the energy conservation principle can be written as

$$C\frac{\partial T}{\partial t} - L\frac{\partial \theta^{(i)}}{\partial t}\rho^{(i)} - \nabla(\lambda\nabla T) = 0 \tag{14}$$

where L is the latent heat of fusion of water per unit mass. It needs to be mentioned that Eq. (14) contains no term due to heat transport by water flow. It also neglects the terms due to mechanical work. These terms are considered small compared to the latent heat released during freezing. The mass conservation principle takes the form

$$\rho^{(s)}\frac{\partial \theta^{(s)}}{\partial t} + \rho^{(w)}\frac{\partial \theta^{(w)}}{\partial t} + \rho^{(i)}\frac{\partial \theta^{(i)}}{\partial t} - \rho^{(w)}\nabla(k\nabla h) = 0 \tag{15a}$$

or

$$(\rho^{(i)} - \rho^{(s)})\frac{\partial n}{\partial t} + (\rho^{(w)} - \rho^{(i)})\frac{\partial (nv)}{\partial t} - \rho^{(w)}\nabla(k\nabla h) = 0 \tag{15b}$$

The momentum conservation principle for the entire mixture (in terms of the total composite stress $\overline{\sigma_{ij}}$) is

$$\frac{\partial \overline{\sigma_{kl}}}{\partial x_l} + \bar{\rho} g_k = 0 \qquad k,l=1,2,3 \tag{16}$$

where g_k is the gravity acceleration vector; and for the skeleton

$$\frac{\partial \overline{\sigma_{kl}^{(s)}}}{\partial x_l} - \rho^{(w)} g_k \nabla h + (\bar{\rho} - \rho^{(w)}) g_k = 0 \qquad k,l=1,2,3 \tag{17}$$

6. Testing for material parameters

Simulation of the freezing processes for specific soils requires that material parameters be known from experimental tests. Reliable techniques for determining material parameters for phenomenological models are those where the material sample tested can be considered a material element. This can be done only if a homogeneous state is introduced to the sample and the response of the material to independently controlled changes in the state parameters can be derived directly from conservation principles. Due to homogeneity of the state parameters the response of every material element in the sample is the same, and the material properties can be calculated easily from the global response of the sample.

Unfortunately, testing the freezing processes re-

quires that the sample be subjected to a temperature gradient, therefore a non-homogeneous response of the material elements throughout the sample must be expected. The contribution of the material in the sample to the global effect (heave of the sample) varies throughout the sample. A feasible way to obtain model parameters, then, is to simulate the freezing processes for which the lab tests were done and try to match the lab results by adjusting the unknown parameters. The number of lab tests (with different boundary conditions) must be at least equal to the number of parameters to be evaluated.

Model parameters such as the unfrozen water content as a function of temperature, hydraulic and thermal conductivity, initial porosity, and densities of the components of the mixture are assumed to be known from independent tests. The parameters of the porosity rate function, however, require some explanation as to their possible methods of estimation. It is suggested that these parameters be derived from tests with "ramped temperatures". Such tests allow a nearly constant temperature gradient to be maintained in the freezing sample, and, thus, the process in the freezing zone can be considered to be approximately stationary with respect to the co-ordinate system attached to the moving freezing front (due to geometrical changes the process is not strictly stationary). As long as the disturbances from the boundary effects are avoided, the heave rate can be expected to be nearly constant (as, for instance, in tests presented by Penner, 1986). Cyclic perturbations in the heave rate need to be expected due to cyclic formation of new ice lenses. These, however, should be neglected when estimating the parameters in the porosity rate function which, by definition, describe the average growth of porosity. It is worthwhile mentioning that when the speed of ramping (rate at which the boundary temperatures are varied) is high, the rate of the freezing front penetration is not proportional to the ramping speed and the process cannot even be considered approximately as stationary. The critical value of the ramping speed depends on the average temperature gradient between the warm and cold boundaries and the heat conductivity.

Parameters can also be evaluated from non-steady freezing processes (e.g., step-freezing), although the overlap of the non-stationary effect and the non-uniform response of the sample to freezing may lead to less accurate results. The heave rate obtained from experiments can be described as

$$\frac{dH}{dt} = \int_0^H \dot{n}_{zz} dz \tag{18}$$

where H is the height of the sample (measured along vertical co-ordinate z), and $\dot{n}_{zz}$ is the respective component of the porosity growth tensor, Eq. (5). Porosity rate for material under a negligible stress state is a function of parameters $\dot{n}_m$, T_m, α, and β, thus a minimum of four tests are needed, each with a different temperature gradient. Parameter ζ needs to be evaluated from additional tests where the sample is loaded with an external load. While, theoretically, five separate tests are needed to evaluate the five parameters, more tests are desirable to obtain a reliable set of parameters. Determining the model parameters then reduces to a curve fitting process with five free parameters. The tests used to determine the parameters must not be used to verify the adequacy of the model.

7. Numerical simulations and sensitivity study

While more work is needed (especially in the area of determining material parameters) before the model can be successfully applied for practical predictions, results of numerical simulations of 1-D freezing processes are presented here to indicate the potential of the model.

A computer program was written to perform the simulations. The program considers the freezing soil an assembly of "control volumes" (or distinct elements) with the heat and mass flow occurring discretely between these volumes. Temperature profiles are linearized between centroids of the control volumes (piece-wise constant temperature gradient). The temperature of the boundary volumes is adjusted to be equal to the prescribed boundary temperatures. The diffusion process inside the "column" is generated numerically through an explicit scheme (independently calculated fluxes between the elements). The number of elements used in

simulations was 40 in the step-freezing process and 20 in the process with ramped temperatures.

7.1. Material parameters

No comprehensive experimental results were found in the literature to allow estimation of all necessary parameters (especially those in the porosity rate function, Eq. (1)). The parameters used in simulations are reasonable estimates adopted for the purpose of presenting qualitative results.

The porosity growth was assumed to be anisotropic with $\xi=1$ (Eq. 5). The first invariant of the stress state in the frozen composite during a 1-D process with anisotropic (one-dimensional) porosity growth was calculated assuming that the frozen composite is elastic

$$\overline{\sigma_{kk}}=\overline{\sigma_z}+2\frac{\mu}{1-\mu}\overline{\sigma_z}=p\frac{1+\mu}{1-\mu} \qquad k=1,2,3 \qquad (19)$$

where $\overline{\sigma_z}$ is the normal vertical component in the total stress tensor (equal to the overburden pressure p; weight of sample neglected), and μ is Poisson's ratio of the frozen composite, assumed here equal to 0.3. The effect of increasing pressure on the walls of the column during 1-D freezing could be modelled by assuming a more realistic value of ξ ($\xi<1$). Laboratory tests are needed to evaluate ξ.

Heat conductivity was assumed as $\lambda=1.7$ W/m °C for unfrozen soil and $\lambda=2.1$ W/m °C for the frozen composite. Heat capacity per unit mass of the skeleton was assumed to be 0.9 kJ/kg °C. Note that increase of porosity in Eq. (1) is described without making use of hydraulic conductivity. The magnitude of the hydraulic conductivity, however, is needed to back-calculate the hydraulic head and cryogenic suction gradient after the frost heave has already been computed. Hydraulic conductivity undergoes large changes in quantity during freezing. Although these changes can be incorporated into the calculations easily, only 2 values of hydraulic conductivity were used: one for unfrozen soil, $k=10^{-2}$ m/24 h, and one for frozen soil, $k=10^{-5}$ m/24 h. The maximum of the porosity rate was assumed as $\dot{n}_m=10$ (1/24 h), and the related temperature as $T_m=-0.15$°C, and $\alpha=0.2$ m/°C and $\beta=5.0$. The parameters in the function representing the unfrozen water content in frozen soil (Eq. 2) were assumed as: $\bar{w}=0.15$, $w^*=0.02$, $a=0.9$ (1/°C), and $T_0=0$°C. The density of the skeleton in the calculations was $\rho_{(s)}=2700$ kg/m^3, and the initial porosity assumed was $n=0.4$.

7.2. Simulation of a step-freezing process

A sample of frost susceptible soil of 0.2 m height was subjected to thermal boundary conditions shown in Fig. 2a. The initial temperature of the entire sample was 1 °C, and at time $t=0$ the temperature of the cold (top) side was dropped to −5 °C, and kept at this level for 20 days. The sample is fully saturated, and the initial total hydraulic head is constant throughout the sample. Figure 3a shows the variation of temperature throughout the sample at different times during the process. The heat flow process becomes almost steady after 2 days (it is not strictly stationary due to the heave process). The variation in the unfrozen water content is shown in Fig. 3b. The initial water content through the entire

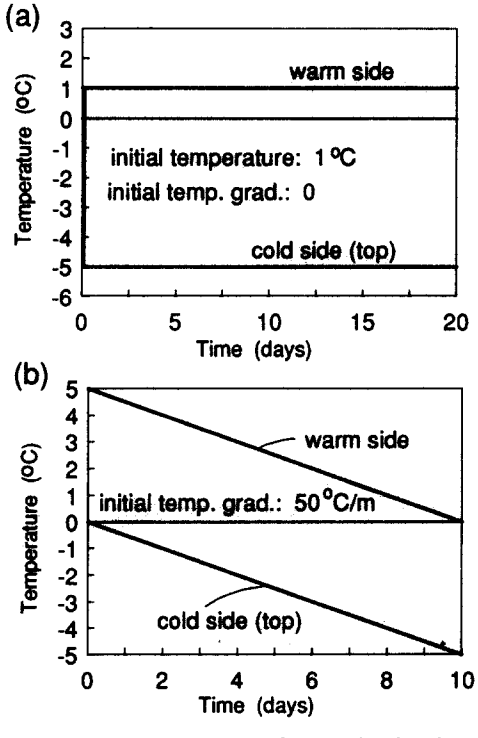

Fig. 2. Boundary conditions for two simulated processes: (a) step-freezing; (b) ramped temperatures.

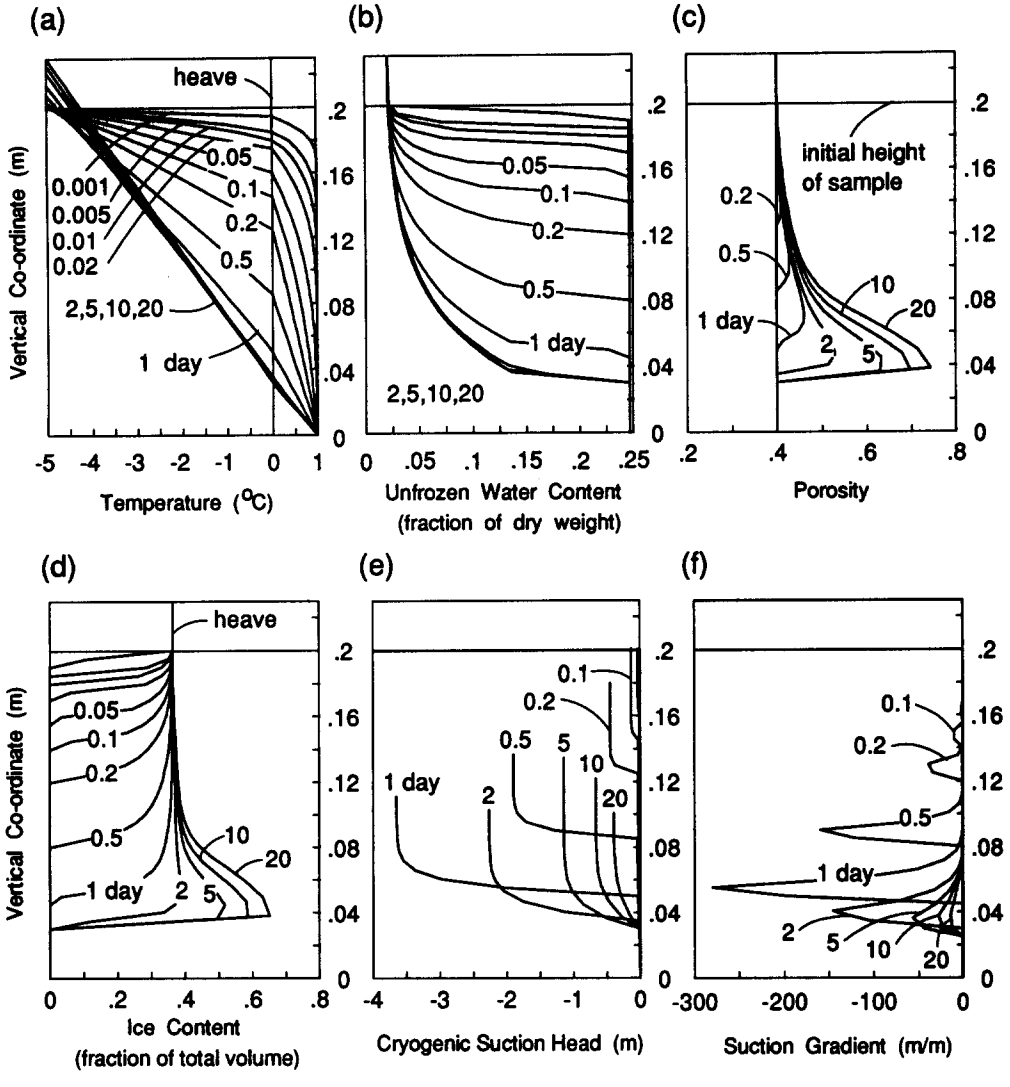

Fig. 3. Step-freezing process: (a) distribution of temperature; (b) unfrozen water content; (c) porosity; (d) ice content; (e) cryogenic suction head; (f) suction gradient.

sample was slightly below 0.25; it drops rapidly around the freezing point, and slowly approaches the value of $w^* = 0.02$. The drop in the unfrozen water content with decreasing temperature affects the heat diffusion process through the release of latent heat.

Increase of porosity and ice fraction is presented in Fig. 3c, d. Appearance of the ice lenses is modelled here as regions of increased porosity, Fig. 3c. The quick advancement of the freezing front in the first four hours of the process results in predominantly freezing in situ where no significant increase in void volume is observed. Once the speed of the 0°C isotherm becomes relatively small, the process of porosity growth becomes very pronounced (Fig. 3c). The ice content increases significantly in the neighborhood of the nearly-stationary freezing zone, which is indicated by the increasing "bulb" in the ice content distribution curves in Fig. 3d. The peak in the ice content distribution can be interpreted as the "final" ice lens formed during step-freezing, while the increased ice content above that indicates

lower average ice concentration, e.g., thinner and widely spaced lenses. Porosity distribution in Fig. 3c is presented in an updated co-ordinate system (taking frost heave into account). Figure 4 shows the same result, but related to the initial height of the sample. It indicates that the "active" porosity growth diminishes rather quickly behind the freezing front.

The expansion of pore volume due to inflowing water in freezing soil is related to the magnitude of the suction gradient. Porosity rate and the hydraulic head gradient are, therefore, two dependent quantities. Once the porosity increase is calculated, the flow rate consistent with this increase can be calculated (saturated soil), and the hydraulic head gradient can be obtained from Darcy's law (Eq. 11). Hydraulic conductivity in frozen soil is very much dependent on temperature (especially in the region of intensive porosity increase), and its exact variation is seldom tested for practical purposes. Back-calculations of the hydraulic head based on approximately estimated hydraulic conductivity are not very accurate, but they are presented here so some qualitative conclusions can be drawn. The variation in elevation head throughout the sample is neglected as small with respect to suction change, thus the gradients calculated from Darcy's law are the pressure (suction) gradients (changes in kinetic head are, of course, neglected too). The suction head and its gradient for the simulated step-freezing process are presented in Fig. 3e, f. The cryogenic suction gradient changes during the process, and it reaches its maximum before a big concentration of increased porosity is formed.

The heave of the sample as a function of time is shown in Fig. 5a. During the step-freezing process the heave rate (derivative of the heave curve) tapers down once the freezing zone becomes almost stationary, and after that it decreases at a much slower pace. Such behavior of the simulated sample is to be expected, since it is postulated in Eq. (1) that the porosity rate decreases with an increase in porosity itself. Application of overburden pressure leads, of course, to a significant decrease in the frost heave. Figure 5a shows the simulated heave curves under different overburden pressures p. Coefficient ζ in the last exponent of Eq. (1) was taken as 300 kN/m^2. For a high overburden pressure the frost heave rate is still significant at the beginning of the process, but it drops down to almost zero in the ad-

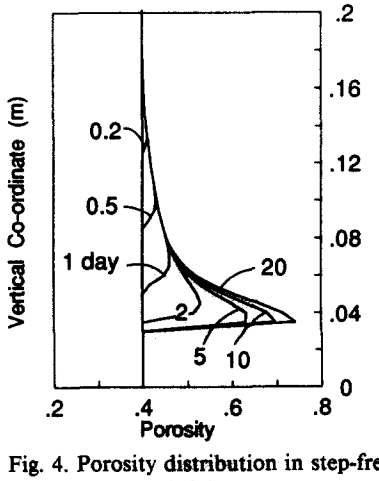

Fig. 4. Porosity distribution in step-freezing process related to initial sample height.

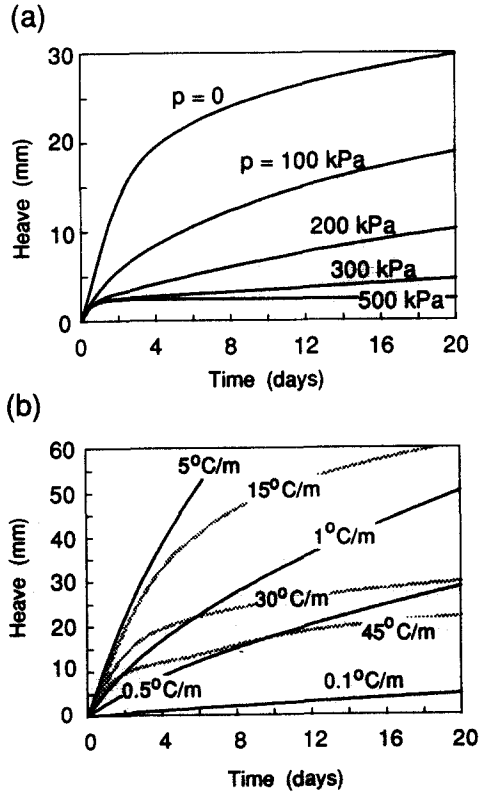

Fig. 5. Frost heave as a function of time in step-freezing processes: (a) influence of overburden pressure; (b) influence of the average temperature gradient.

vanced stage. For an overburden pressure of $p=2$ MN/m^2, the total heave after 20 days was zero, for all practical purposes.

7.3. Simulation of a freezing process with ramped temperatures

The soil is now assumed less frost susceptible, maximum porosity rate $\dot{n}_m$ is equal to 2.0 (1/24 h), and the height of the sample is 10 cm (all other parameters the same). The thermal boundary conditions are presented in Fig. 2b. The temperature and the unfrozen water distribution are shown in Fig. 6a, b. An initially constant temperature gradient displays a gentle change at the freezing front (0°C isotherm) as the heat conductivity was assumed different for the frozen and unfrozen soil. As propagation of the freezing front becomes almost steady in the advanced process, the porosity increase left behind the freezing zone is nearly constant, Fig. 6c. The distinct change in the ice content behind the freezing front, Fig. 6d, is caused by freezing in situ according to the relation in Eq. (6). The cryogenic suction head and its gradient at the freezing front are nearly constant in the advanced freezing process, Fig. 6e, f. The frost heave of the sample takes

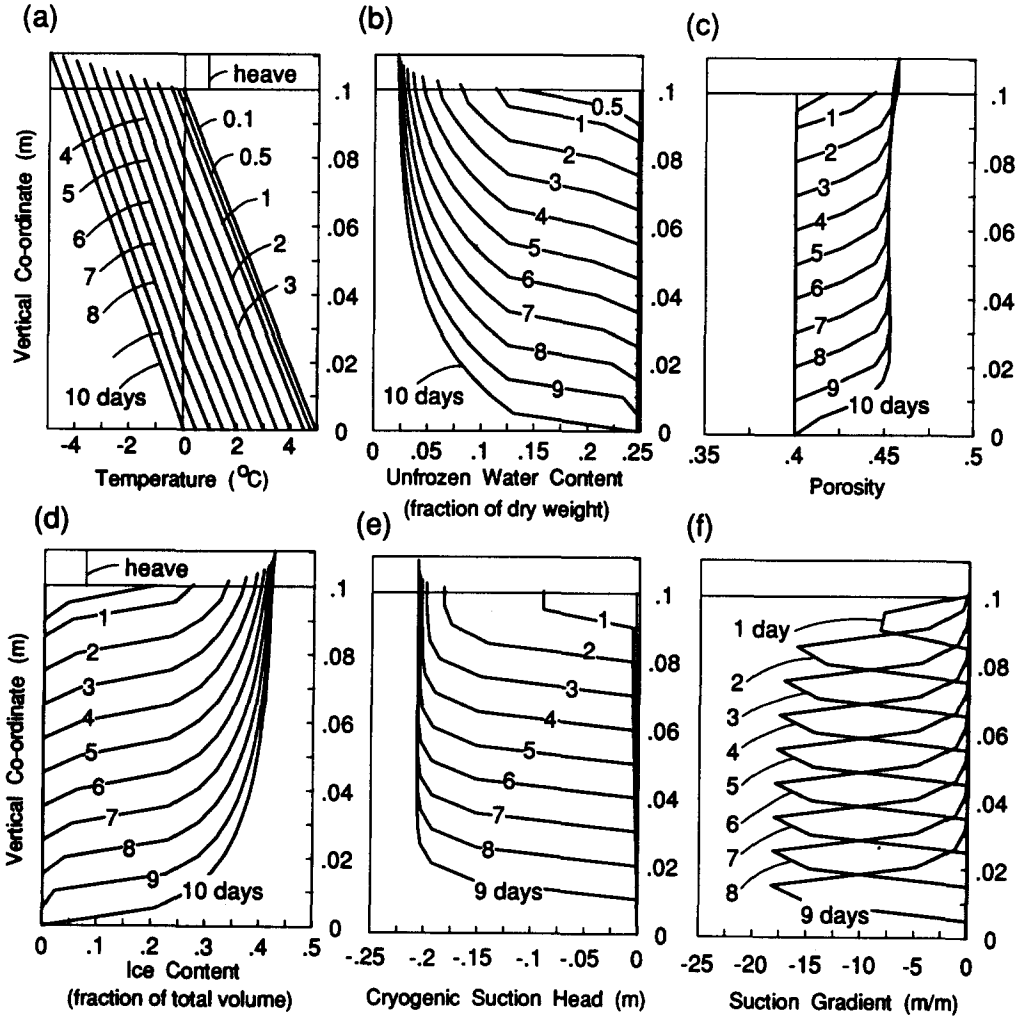

Fig. 6. Freezing process with ramped temperatures: (a) distribution of temperature; (b) unfrozen water content; (c) porosity; (d) ice content; (e) cryogenic suction head; (f) suction gradient.

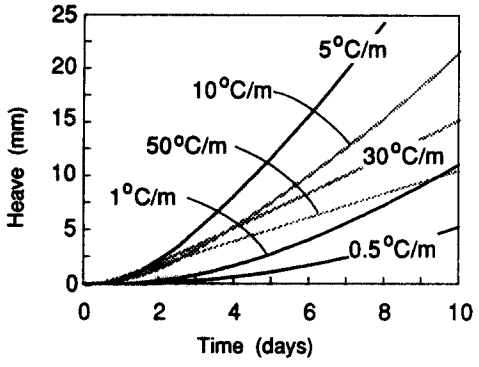

Fig. 7. Frost heave as a function of time for different average temperature gradients in freezing processes with ramped temperatures.

place at an almost constant rate, except for the first day of the process (heave-time relation for temperature gradient of 50°C/m in Fig. 7).

7.4. Sensitivity of frost heave to crucial parameters

Detailed parametric analysis indicating how sensitive frost heave is to all model parameters would lead to a rather lengthy report and is beyond the scope of this paper. This study indicates, however, the influence of the most crucial parameters on the predictions of frost heave, but is not meant to be a comprehensive sensitivity analysis. The crucial parameters are: maximum porosity rate $\dot{n}_m$, parameter α, describing sensitivity of the model to the temperature gradient, initial porosity, n, and parameter β, characterizing the influence of porosity increasing during a freezing process. Porosity increase is related to the flux of water into the freezing soil; therefore, once the porosity rate is calculated from Eq. (1), the hydraulic conductivity must not be an independent parameter. Hence, the hydraulic conductivity needs to be considered as being included in the porosity rate function (Eq. 1) implicitly through other material parameters, and, it is not placed among the critical parameters influencing the calculations of frost heave here. To indicate the influence of the crucial parameters on frost heave, step-freezing processes of 20 cm tall samples were simulated with boundary conditions as in Fig. 2a, and with material parameters $\dot{n}_m$, α, n, and β varied. The basic set of parameters is the same as described in Section 7.1, and only one parameter will vary from that set in each simulation here.

Parameter $\dot{n}_m$ is very critical in predictions of frost heave. An extensive laboratory program needs to be carried out to estimate reliable values of $\dot{n}_m$. Simulations of freezing processes for which lab test results are known led to reasonable results when $\dot{n}_m$ was as small as 0.40 (1/24 h) for a soil mix of moderate frost susceptibility (Penner, 1986), 15 (1/24 h) for Devon silt (described by Konrad and Morgenstern, 1980, as highly frost susceptible), and as much as 500 (1/24 h) for a very frost susceptible mixture of ground chalk and sand (McCabe and Kettle, 1985). Results of frost heave simulations for three values of $\dot{n}_m$ are shown in Fig. 8a. The larger the value of $\dot{n}_m$, the larger the frost heave. The dependence is almost linear in the range shown, i.e., a constant increase in $\dot{n}_m$ produces an almost constant increase in the total frost heave after 20 days. One would expect this relation to be close to linear as the porosity rate is proportional to $\dot{n}_m$ (Eq. 1, see also Fig. 1a). The slight deviation from linearity is caused by the influence of the porosity itself and the variation in temperature gradient due to different heave (although the latter has a minor effect as long as the heave is small with respect to the sample height).

The influence of coefficient α is captured in Fig. 8b. This influence is, of course, exponential (see Eq. 1 and Fig. 1b). Finally, the influence of the initial porosity and coefficient β are illustrated in Figs. 8c and d (see also Fig. 1c). The larger the initial porosity, the lower the frost heave. Coefficient β has a very profound effect on the magnitude of frost heave. It was found from simulations of different freezing processes for different soils (Michalowski, 1992, 1993) that the frost heave curves are very realistic when the value of β is around 5 for all soils. Thus, parameter $\dot{n}_m$ defined as the maximum porosity rate is far greater than the maximum porosity rate possible in a soil. This is because the coefficient $(1-n)^\beta$ in Eq. (1) attains quite small values, e.g., when the porosity changes from 0.3 to 0.6 this coefficient changes from about 0.17 to 0.01.

The influence of the overburden pressure had already been illustrated earlier (Fig. 5a). The increasing stress hinders the formation of new ice lenses modelled as an increase in porosity. Based on

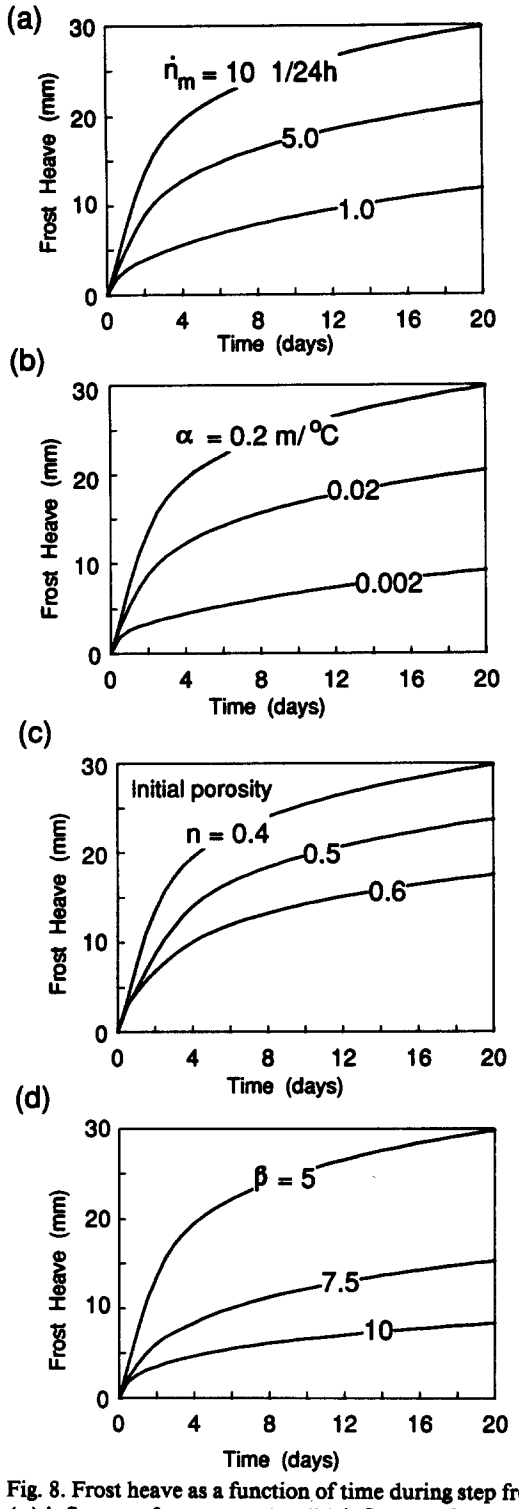

Fig. 8. Frost heave as a function of time during step freezing: (a) influence of parameter $\dot{n}_m$; (b) influence of parameter α; (c) influence of the initial porosity; (d) influence of parameter β.

lab tests by Konrad and Morgenstern (1982), a reasonable value of parameter ζ was found to be about 300 kN/m^2. This may, of course, be different for different soils. When the overburden pressure, p, is beyond 300 kN/m^2, a significant rate of heave occurs only at the very beginning of the process, and, when p is in the range of MN/m^2 (megapascals), the heave becomes zero, for all practical purposes.

The influence of the temperature gradient on frost heave is shown in Fig. 7 and Fig. 5b in the process with ramped temperatures and in the step-freezing process, respectively. The temperature gradient is not a material property, nevertheless its influence is shown here as it relates to the rate of heat extraction and the rate of cooling, often given as parameters affecting frost heave. Neither heat extraction rate nor the cooling rate are material parameters and as such, they cannot influence the model of the material (frost susceptible soil) itself. It is crucial in interpreting the results of simulations (and also in interpreting the lab experiments) that the total response of the sample to specific boundary conditions not be mixed with local response of the soil to freezing. The line for temperature gradient 50°C/m in Fig. 7 shows frost heave as a function of time for boundary conditions as in Fig. 2b. All other processes were simulated with the initial temperature of the warm side lower, such that the average gradient in the sample was as indicated for curves in Fig. 7. In all cases the temperature of the warm side was dropped to 0°C in 10 days, and the initial temperature of the cold side was 0°C. At the very beginning of all freezing processes the rate of heave is the lowest. This is because the freezing front has just entered the sample, and the volume of soil in which the porosity increases is small. Hence, the integral of the rate of volume growth is also small. It increases, however, once the freezing front advances and, for a large temperature gradient (50°C/m), becomes constant through the rest of the process. In this case the freezing process can be considered stationary with respect to the propagating freezing front. The frost heave of the sample is relatively low for a very small average temperature gradient of 0.5°C/m. It becomes higher with an increase in the average temperature gradient, and it drops again for very large gradients. It should be noted that for gradients up to 5°C/m the rate of freezing front pene-

tration was not proportional to the rate of ramping. The drop in the frost heave for very large gradients is not surprising, since, the larger the gradient, the smaller the part of the sample responding with a significant porosity increase. The ramping rates were defined for the warm and cold sides of the sample, thus the temperature gradient through the sample had a tendency to decrease due to increasing sample height.

A similar tendency can be seen in the step-freezing process (Fig. 5b). Here, all samples were subjected to boundary conditions qualitatively similar to those in Fig. 2a, but with temperatures assuring the average gradients as in Fig. 5b. The ratio of the warm to the cold plate temperature was equal to $-1/5$ in all cases. Note that the true temperature gradients throughout samples during the freezing process are different from the average ones indicated in Fig. 5b (first due to the non-steady energy transfer, and later in the process due to an increase in the sample height, and nonuniform thermal conductivity).

The heave of the sample increases with an increase in the temperature gradient, but, again, for very large gradients, it decreases (Fig. 5b). For very small temperature gradients (and a temperature below freezing but above T_m) the local porosity increase is low according to Eq. (1), and frost penetration is slow. Increase in the average temperature gradient results in a greater volume increase. When the average gradient is very high, however, the sample is being "shock frozen" with a small porosity increase in its top part (Fig. 3c), but with fast moving frost front (freezing in situ). The rate of frost heave is high in this initial stage of freezing, but it tapers down once the frost front reaches an almost stationary position after the first 2–3 days (curves for 30 and 45°C/m in Fig. 5b).

8. Final remarks

The model presented is not derived from micromechanical processes, and it is not targeted at explaining the frost heave phenomenon, but it is focused at qualitative and quantitative predictions of frost heave in saturated soils. The model considers soil a porous medium, with pores filled with water, or water and ice. Volumetric changes occur due to porosity increase, which is caused by the inflowing and freezing water driven by cryogenic suction. The process of the formation of discrete ice lenses is "smeared" over a representative volume, and simulated by the porosity increase of the mixture.

The model hinges on introducing a porosity rate function as the characteristic material property of frost susceptible soils. Hypothetical dependencies of the void increase due to temperature, temperature gradient, current magnitude of porosity, and the stress state need further experimental verification. While raw data available in the literature do not allow verification of the model, the simulations of step-freezing processes and processes with ramped temperatures indicate very realistic (qualitatively) behavior of soil under freezing conditions.

Acknowledgement

The research presented here was supported by the Underground Space Center and The Center for Transportation Studies of the University of Minnesota.

References

Anderson, D.M. and Tice, A.R., 1973. The unfrozen interfacial phase in frozen water systems. In: A. Hadar (Editor), Ecological Studies: Analysis and Synthesis. Vol. 4, pp. 107–124.

Beskow, G., 1935. Soil freezing and frost heaving with special application to roads and railroads. The Swedish Geological Society, Series C, 375 pp. (translated by J.O. Osberberg; published by Technical Institute, Northwestern University, 1974).

Black, P.B. and Miller, R.D., 1985. A continuum approach to modelling frost heaving. In: D.M. Anderson and P.J. Williams (Editors), Freezing and Thawing of Soil–Water Systems. ASCE, pp. 36–45.

Blanchard, D. and Frémond, M., 1985. Soil frost heaving and thaw settlement. In: S. Kinosita and M. Fukada (Editors), 4th Int. Symp. Ground Freezing, Sapporo. Balkema, Rotterdam, pp. 209–216.

Burt, T.P. and Williams, P.J., 1976. Hydraulic conductivity in frozen soils. Earth Surf. Processes, 1: 349–360.

Everett, D.H., 1961. The thermodynamics of frost damage to porous solid. Trans. Faraday Soc., 57: 1541–1551.

Frémond, M., 1987. Personal communication.

Guymon, G.L., Hromadka, T.V. and Berg, R.L., 1984. Two-dimensional model of coupled heat and moisture trans-

port in frost-heaving soils. J. Energy Resour. Technol., 106: 336–343.

Holden, J.T., 1983. Approximate solutions for Miller's theory of secondary heave. In: Fourth Int. Conf. Permafrost, Fairbanks, AK, pp. 498–503.

Holden, J.T., Piper, D. and Jones, R.H., 1985. Some developments of a rigid-ice model of frost heave. In: S. Kinosita and M. Fukada (Editors), 4th Int. Symp. Ground Freezing, Sapporo. Balkema, Rotterdam, pp. 93–99.

Konrad, J.M. and Morgenstern, N.R., 1980. A mechanistic theory of ice lens formation in fine-grained soils. Can. Geotech. J., 17: 473–486.

Konrad, J.M. and Morgenstern, N.R., 1982. Effects of applied pressure on freezing soils. Can. Geotech. J., 19: 494–505.

Konrad, J.M. and Morgenstern, N.R., 1984. Frost heave prediction of chilled pipelines buried in unfrozen soils. Can. Geotech. J., 21: 100–115.

Li, Y., Michalowski, R.L., Dasgupta, B. and Sterling, R.L., 1989. Preliminary results from simulation of retaining wall displacement by frost action. In: R.L. Michalowski (Editor), 5th Int. Conf. Cold Regions Engineering. ASCE, New York, pp. 389–396.

McCabe, E.Y. and Kettle, R.J., 1985. Thermal aspects of frost action. In: 4th Int. Symp. on Ground Freezing, Sapporo, pp. 47–54.

Michalowski, R.L., 1992. A constitutive model for frost susceptible soils. In: G.N. Pande and S. Pietruszczak (Editors), Proc. 4th Int. Symp. Numerical Models in Geomechanics, Swansea. Balkema, Rotterdam, pp. 159–167.

Michalowski, R.L., 1993. Phenomenological modelling of frost-susceptible soils. In: Proc. VI Int. Conf. Permafrost, Beijing.

Miller, R.D., 1978. Frost heaving in non-colloidal soils. In: Proc. Third Int. Conf. Permafrost, Edmonton, Alberta, pp. 707–713.

Nixon, J.F., 1987. Thermally induced heave beneath chilled pipelines in frozen ground. Can. Geotech. J., 24: 260–266.

O'Neill, K. and Miller, R.D., 1980. Numerical solutions for a rigid ice model of secondary frost heave. In: 2nd Int. Symp. Ground Freezing, Trondheim, pp. 656–669.

O'Neill, K. and R.D. Miller, R.D., 1985. Exploration of a rigid ice model of frost heave. Water Resour. Res., 21: 281–296.

Penner, E., 1959. The mechanism of frost heaving in soils. Highw. Res. Board Bull., 225: 1–22.

Penner, E., 1986. Aspects of ice lens growth in soils. Cold Reg. Sci. Technol., 13: 91–100.

Römkens, M.J.M. and Miller, R.D., 1973. Migration of mineral particles in ice with a temperature gradient. J. Colloid Interface Sci., 42: 103–111.

Shen, M. and Ladanyi, B., 1987. Modelling of coupled heat, moisture and stress field in freezing soil. Cold Reg. Sci. Technol., 14: 237–246.

Taber, S., 1929. Frost heaving. J. Geol., 37: 428– 461.

Taber, S., 1930. The mechanics of frost heaving, J. Geol., 38: 303–317.

Williams, P.J. and Wood, J.A., 1985. Internal stresses in frozen soil. Can. Geotech. J., 22: 413–416.